Effect of Water on the Local Structure and Phase Behavior of Imidazolium-Based Protic Ionic Liquids

ARTICLE *in* THE JOURNAL OF PHYSICAL CHEMISTRY B · DECEMBER 2014

Impact Factor: 3.3 · DOI: 10.1021/jp510691e · Source: PubMed

4 AUTHORS, INCLUDING:

Negin Yaghini
Chalmers University of Technology
5 PUBLICATIONS **18** CITATIONS

SEE PROFILE

Aleksandar Matic
Chalmers University of Technology
109 PUBLICATIONS **1,637** CITATIONS

SEE PROFILE

Anna Martinelli
Chalmers University of Technology
32 PUBLICATIONS **729** CITATIONS

SEE PROFILE

THE JOURNAL OF PHYSICAL CHEMISTRY B

Article

pubs.acs.org/JPCB

Effect of Water on the Local Structure and Phase Behavior of Imidazolium-Based Protic Ionic Liquids

Negin Yaghini,[‡] Jagath Pitawala,[¶] Aleksandar Matic,[§] and Anna Martinelli*[,‡]

[‡]Department of Chemistry and Chemical Engineering and [§]Department of Applied Physics, Chalmers University of Technology, 41296 Gothenburg, Sweden

[¶]Department of Science and Technology, Uva Wellassa University, Badulla, Sri Lanka

Supporting Information

ABSTRACT: We report on the effect of water on local structure and phase behavior of two protic ionic liquids, C_2HImTFSI and C_2HImTfO. Raman and infrared spectroscopy are employed to investigate the local coordination state. We find that water interacts weakly with $TFSI^-$ while more specifically with TfO^- through the $-SO_3$ group. Additionally, we observe that upon addition of water the −NH stretching frequency does not change in C_2HImTFSI, while it red-shifts in C_2HImTfO, indicative of different hydrogen bonding configurations. Supported by the appearance of some additional features in the 800−1000 cm^{-1} frequency range where ring out-of-plane bending (γ) modes are found, we hypothesize that in C_2HImTFSI water interacts only with the cation coordinating to the ring C^2H and the N^3H sites, while it interacts with both cation and anion in C_2HImTfO forming hydrogen bonds that involve the cationic N−H site as well as the anionic $-SO_3$ group. These different local structures also reflect in the phase behavior investigated by DSC, which reveals a more homogeneous solution when water is added to C_2HImTfO, as compared to H_2O/C_2HImTFSI mixtures. Finally we report that the addition of water also significantly affects both T_m and T_g.

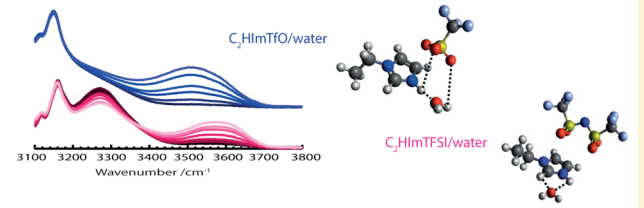

In this study we investigate the effect of adding water on local structure and phase behavior in two protic ionic liquids.

INTRODUCTION

Protic ionic liquids (PILs) constitute a subset of ionic liquids that, differently from their aprotic counterparts, possess exchangeable protons.[1] Thus, besides providing the beneficial properties of low volatility,[2] nonflammability, high conductivity, and chemical stability, PILs are also prone to forming extended hydrogen bonded networks, which become favorable in diverse applications.[1] One application where this is advantageous is the proton exchange membrane fuel cell (PEMFC). In fact, the archetypical PEM material is a perfluorinated polymer membrane (Nafion, a trademark of E. I. du Pont de Nemours and Company) that displays superior performance at high hydration and low temperatures but shows drastic conductivity drops at around 80 °C due to the evaporation of water.[3] As a consequence, by virtue of being nonvolatile and good proton conductors PILs are suitable candidates for PEMFC applications also at higher temperatures. However, although the original idea was to find anhydrous alternatives to water-based PEMs, more recently the research has moved toward the deliberate addition of water to PILs,[4]since this has been revealed to increase the ionic conductivity,[5] decrease the viscosity,[6−8] and improve the overall fuel cell performance.[9−12] In this context, it is important to mention that the water produced at the cathode of a fuel cell can back-diffuse and mix with the ionic liquid already present in the PEM. Moreover, the exact mechanism of proton conduction in PILs is at present not thoroughly understood, even though a proton hopping mechanism between protic cations and water has been speculated to occur.[13] As a consequence, there is a need to better understand how the presence of water affects the intrinsic properties of PILs, from both a fundamental and an applied viewpoint. In particular, it is crucial to understand the correlation between local structure and transport properties in H_2O/PIL binary systems.

Molecular dynamic (MD) simulations on *N,N*-diethyl-*N*-methylammonium triflate [dema:TfO] and its mixtures with water, and experimental work on the mixtures of 1-butyl-3-methylimidazolium hexafluorophosphate, [bmim][PF_6], 1-butyl-3-methylimidazolium tetrafluoroborate, [bmim][BF_4], and 1-butyl-3-methylimidazolium trifluoroacetate, [bmim]-[CF_3CO_2] with water, have shown that when water is added at very small concentrations it situates at interstitial sites between the anion and the cation, mainly coordinating to the anion and disrupting the cation−anion association.[14,15] In particular, the MD simulations performed by Chang et al. for higher concentrations, up to an equivalent of 0.5 water molecules per cation−anion pair, indicate that these are isolated from each other, while only for concentrations above 0.8 can water molecules form a bulk-like network.[14] In addition, nuclear magnetic resonance (NMR) spectroscopy and vibra-

Received: October 24, 2014
Revised: December 28, 2014
Published: December 30, 2014

DOI: 10.1021/jp510691e
J. Phys. Chem. B 2015, 119, 1611−1622

tional spectroscopic measurements on aqueous 1-decyl-3-methyl-imidazolium bromide, [C_{10}mim][Br], have also revealed different states of water depending on the relative concentration, namely, loosely bonded water, water taking part in the hydrogen-bond exchange process, and water molecules in more regular structures.[16] The existence of different types of water has also been discussed by Fazio et al., who by inspecting the vibrational changes in the spectral range for O−H and B−F stretching distinguish between network and intermediate water in mixtures of H_2O and 1-butyl-3-methyl-imidazolium tetrafluoroborate, [C_4C_1Im][BF_4].[17] Similar results have been reported by Takamuku et al., who have investigated by infrared spectroscopy the nature of water in 1-ethyl-3-methylimidazolium tetrafluoroborate, [C_2C_1Im][BF_4].[18]

Our recent investigation by ^{1}H NMR of imidazolium based protic and aprotic ionic liquids associated with the trifluoromethanesulfonate (TfO) or the bis(trifluoromethanesulfonyl)-imide (TFSI) anion, i.e., [C_2HIm][TFSI], [C_2C_1Im][TFSI], [C_2HIm][TfO], and [C_2C_1Im][TfO],[5] has shown that the effect of water on the transport properties strongly depends on the specific cation/anion combination, suggesting that the protonation of the cation has a deep impact on the nature of the H_2O−IL interaction. In that study, we hypothesized a specific interaction through the −NH group of the imidazolium ring, and observed stronger perturbations in the systems based on the TfO anion as compared to those based on TFSI.[5] Our results also suggested that the addition of water can affect the 'ionicity' of the PIL, an important aspect with respect to the use of PILs as electrolytes.

To get further insights into these issues we now investigate the local structural changes induced by added water and aim to elucidate the relative position of cations, anions, and water molecules. We therefore focus on the same PILs as in ref 5, that is on 1-ethylimidazolium bis(trifluoromethane-sulfonyl)imide, [C_2HIm][TFSI], and 1-ethylimidazolium trifluoromethanesulfonate, [C_2HIm][TfO], but now employing vibrational spectroscopy, including both infrared and Raman, to investigate the nature of intermolecular interactions in the pure and water-added ionic liquids. More specifically, while infrared (IR) spectroscopy is most suitable to investigate the H_2O−C_2HIm^+ interactions by being sensitive to both O−H and N−H stretching vibrations, Raman spectroscopy is more appropriate to study the H_2O−anion interactions since the vibrations of the SO_2/SO_3 and CF_3 groups present in TfO and TFSI have strong Raman intensities, while they are both weak and interfering with cation signatures in infrared. Finally, to relate the local structure with the macroscopic properties, we also analyze the effect of water on the phase behavior of these PILs using differential scanning calorimetry (DSC).

EXPERIMENTAL SECTION

Materials. 1-Ethylimidazolium trifluoromethanesulfonate (C_2HImTfO) and 1-ethylimidazolium bis-(trifluoromethanesulfonyl)imide (C_2HImTFSI) were purchased from Io.Li.Tec Germany and stored in a glovebox prior to use. The water content of the purchased ionic liquids was analyzed by Karl Fischer experiments and estimated to be 57 ppm for C_2HImTFSI and 237 ppm for C_2HImTfO (which correspond to approximately one-tenth of the smallest amount of deliberately added water). The cationic and anionic molecular structures, along with the carbon and nitrogen atoms labeling used in this work, are shown in Figure 1. H_2O/IL mixtures were prepared with different H_2O-to-IL mole ratios, x, with x varying in the range $0 \leq x \leq 1$, more specifically x = 0, 0.05, 0.1, 0.2, 0.4, 0.6, 0.8, and 1.0. H_2O/IL samples were analyzed immediately after preparation.

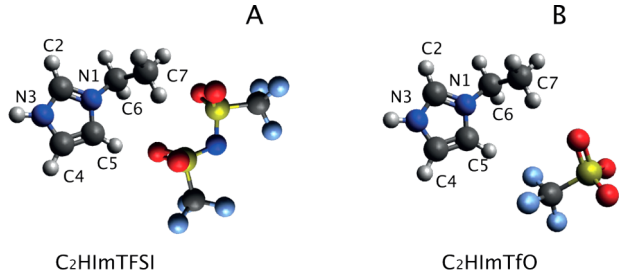

Figure 1. Molecular structure and acronym for the investigated protic ionic liquids: 1-Ethylimidazolium bis(trifluoromethanesulfonyl)imide, C_2HImTFSI (A), and 1-Ethylimidazolium trifluoromethanesulfonate, C_2HImTfO (B). Carbon and nitrogen labeling of the cation is also shown.

Differential Scanning Calorimetry. Differential scanning calorimetry (DSC) experiments were performed in the temperature range −120 to +50 °C, in hermetically sealed aluminum pans. Samples containing the pure ionic liquids were prepared in an argon filled glovebox. The samples were first cooled from 40 °C to −120 °C at a rate of 20 °C/min, while the DSC traces were recorded during the subsequent heating, with a scan rate of 10 °C/min, up to 50 °C for C_2HImTfO, and to 30 °C for C_2HImTFSI (due to the higher melting point, the heating scan for C_2HImTfO was performed up to 50 °C). The rapid cooling is performed to prevent crystallization and thus possibly detect a glass transition during the heating scan. As a confirmation of the reproducibility of the experiment two cycles of cooling/heating scans were performed, but only the data from the second scan are used here for analysis.

Vibrational Spectroscopy. *Infrared Spectroscopy.* Infrared spectra were collected with a PerkinElmer 2000 FT−IR spectrometer using the attenuated total reflection (ATR) mode and pouring the solutions over a ZnSe crystal. For each sample, 32 scans were averaged and the resolution was 2 cm^{-1}. A pyroelectric detector (MIR TGS) sensitive from 650 to 4000 cm^{-1} was used to convert the IR radiation to electrical signal.

Raman Spectroscopy. Raman spectra were recorded with a InVia Reflex Renishaw spectrometer. The 785 nm line of a diode laser was used as the excitation source. The laser was set to 50% of full power, which is nominally 300 mW at the source. The spectral resolution was 2 cm^{-1}. Recorded spectra were accumulated by 4 scans, with a duration of 10 s each. Raman spectra were recorded at room temperature. In order to analyze the Raman and IR spectra in deeper detail, a peak-fit procedure based on a linear combination of Voigt or Gaussian profiles and a linear background was employed to model the spectral ranges where relevant molecular vibrations were observed. The number of fitting components was limited to the number of normal modes of vibration predicted by theoretical calculations available in the literature.[17,19,20]

RESULTS AND DISCUSSION

Preamble: Vibrational Spectroscopy as a Tool To Investigate Cation−Anion Interactions. Before going deeper into the effect of water on the intermolecular interactions in the PILs C_2HImTFSI and C_2HImTfO, it is important to make some assumptions on the relative orientation that the constituting cations and anions may

DOI: 10.1021/jp510691e
J. Phys. Chem. B 2015, 119, 1611−1622

adopt. A smart way to deduce this in similar imidazolium ionic liquids has recently been discussed by Cha et al.,[19] and is based on the analysis of frequency changes induced by the addition of water in the infrared spectral range 2700−3200 cm^{-1} where both ring and alkyl chain −CH stretching modes are found. This approach is very similar to the one that we aim to employ in this study, although we focus here on protic ionic liquids (rather than aprotic) and also complement with an analysis of the anion's state by Raman spectroscopy, and of the nature of water by IR spectroscopy.

The IR spectra of the PILs C_2HImTFSI and C_2HImTfO are shown in Figure 2 together with the spectra recorded for their

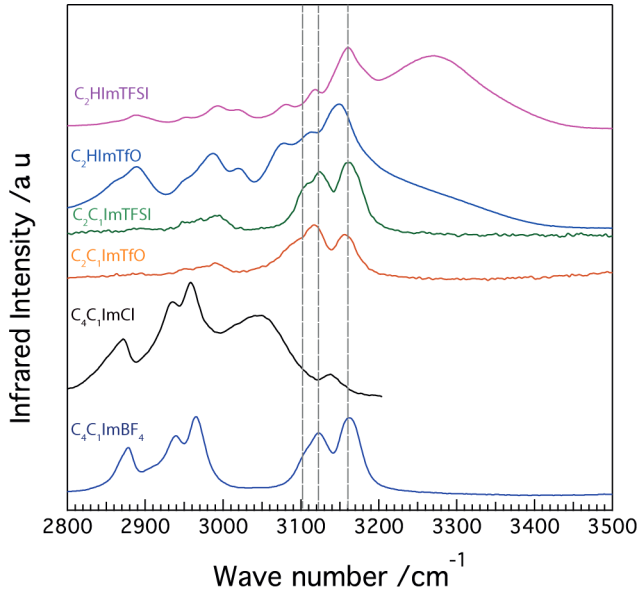

Figure 2. High frequency range of IR spectra of (from bottom to top) pure $C_4C_1ImBF_4$, C_4C_1ImCl (reproduced with permission from ref 19), C_2C_1ImTfO, $C_2C_1ImTFSI$, $C_2HImTfO$, and $C_2HImTFSI$. The approximate frequencies of the ring C^4−H, C^5−H, and C^2−H stretching modes are indicated by vertical lines.

aprotic analogues, i.e., $C_2C_1ImTFSI$ and C_2C_1ImTfO, and that recorded by Cha et al. for the aprotic ILs 1-butyl-3-methylimidazolium tetrafluoroborate ($C_4C_1ImBF_4$) and 1-butyl-3-methylimidazolium chloride (C_4C_1ImCl) reproduced with permission from ref 19. This figure reveals that the vibrational spectra of the aprotic ionic liquids are very similar to each other and to that of $C_4C_1ImBF_4$, in terms of frequency of the ring C^4−H, C^5−H, and C^2−H stretching modes, indicated by vertical lines (see also Table 1), which are known to be sensitive to the strength of the cation−anion interaction through hydrogen bonding.[19,21] This similarity, concomitantly with the very little effect observed on the frequency of these vibrations upon addition of water (spectra not shown here), suggests that the C_2C_1Im cation interacts weakly and nonspecifically with both TFSI and TfO, similarly to the case of $C_4C_1ImBF_4$ already discussed in ref 19.

Interestingly, the spectra of the PILs C_2HImTFSI and C_2HImTfO show small red-shifts for $C^{2,4,5}$−H vibrations (Table 1), indicating that the cation−anion pairs are only slightly closer than in the aprotic analogues.[19] This reflects in higher melting temperatures for these PILs (see Table 1), and is in line with the findings recently discussed by Fumino et al., who also found by vibrational spectroscopy that protonation of the N sites on the imidazolium ring does affect the nature of cation−anion association.[22]

Thus, in analogy to the conclusions drawn for the ionic liquid C_4C_1ImBF4[19] we assume here that in both C_2HImTFSI and C_2HImTfO the anions are located somewhere above the imidazolium ring rather than on its plane (note: the latter, on the other hand, is the structure assumed in aprotic ILs of the type $C_4C_1Im^+X^-$, where X^- is an halide anion;[19] in particular, this local structure reflects in a very different infrared spectrum with a considerable red-shift of the ring CH stretching modes; see, for instance, C_4C_1ImCl in Figure 2 (also Figure 1 in ref 19)). This assumption becomes very important with respect to the interpretation of the spectroscopic data that will be developed further in the next sections. In addition, we can anticipate here that the broader signatures observed above 3200 cm^{-1} in the IR spectra of both C_2HImTFSI and C_2HImTfO are due to the N−H stretching mode, which can also be used as an indicator of the interaction strength between the C_2HIm^+ cation and the anion or, in the binary systems, between the C_2HIm^+ cation and water.

Vibrational Modes of the Anions. The characteristic vibrations of the TFSI and the TfO anions are best investigated in the Raman spectrum, where they appear intense and well separated from the contributions due to the cation. More specifically, the most intense Raman feature for TFSI is found at 743 cm^{-1} in C_2HImTFSI and is assigned to the expansion−contraction mode of the whole molecule with strong contributions from the bending mode of the CF_3 group; see

Table 1. Melting Temperature, Frequency, and Assignment of the Ring CH Stretching Modes Observed in the Protic and Aprotic Imidazolium Ionic Liquids[a]

Assignment[19]	$C_4C_1ImBF_4$	C_2C_1ImTfO	$C_2C_1ImTFSI$	$C_2HImTfO$	$C_2HImTFSI$
T_m	−75 °C	−10.4 °C	−9.8 °C	27 °C	7 °C
ν_s CH_2	2856				
ν_{as} CH_2	2913				
ν_s CH_3	2877			2889	2888
ν_{as} CH_3	2965	2957	2953	2989	2993
ν_s NCH_3	2985	2991	2991	3022	3016
ν_{as} NCH_3	3036	3060	3098		
ν C^2H	3114	3097	3107	3070	3082
ν_{as} C^4HC^5H	3120	3120	3127	3109	3116
ν_s C^4HC^5H	3163	3157	3162	3149	3159

[a]The corresponding values for the aprotic ionic liquid $[C_4C_1Im][BF_4]$, a.k.a $[bmim][BF_4]$,[19] are also included in this table. The superscript numbers in C^2, C^4, and C^5 are used to denote carbon labeling according to Figure1.

DOI: 10.1021/jp510691e
J. Phys. Chem. B 2015, 119, 1611−1622

Figure 3. This frequency is slightly higher than for the aprotic ionic liquid (~740 cm^{-1}), in agreement with a stronger cation−

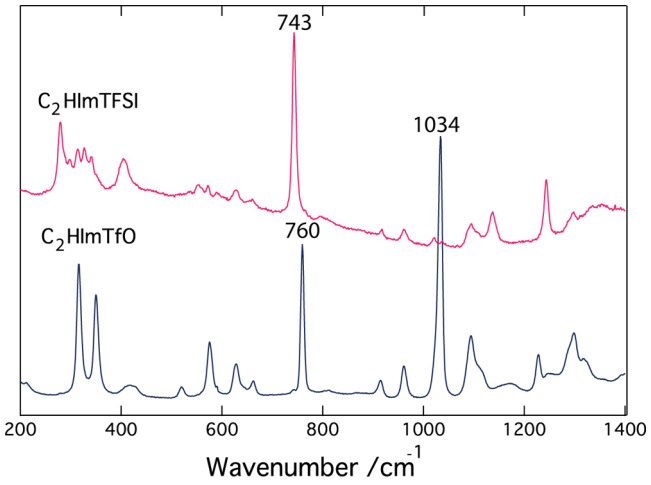

Figure 3. Raman spectra of pure C_2HImTFSI and C_2HImTfO.

anion interaction, as discussed above, and in particular with the red-shifted C[2,4,5]−H stretching modes. The TFSI anion displays characteristic Raman features also in the low-frequency range 240−430 cm^{-1} (Table 2), which is sensitive to conformational changes and contains contributions from the rocking (ρ) and twisting (τ) of the CF_3 and SO_2 groups. Indeed, the two conformations that TFSI can adopt, i.e., the cisoid (*cis*, C_1 symmetry) and the transoid (*trans*, C_2 symmetry), can be distinguished in this spectral region by relative peak intensities, as investigated by a few authors for diverse TFSI-based ionic liquids.[20,26]

Table 2. Observed Vibrational Modes in the Raman Spectra of C_2HImTfO and C_2HImTFSI, Recorded at Room Temperature[a]

C_2HImTfO			C_2HImTFSI		
ω (cm^{-1})	assignment	ref	ω (cm^{-1})	assignment	ref
			278m	$\rho(CF_3)$	23
			296m	$\rho(CF_3)$, $\nu_{as}(CS)$ (transoid)	23
315s	ν(C−S)	24, 25	314m	$\rho(SO_2)$, $\rho(CF_3)$ (transoid), $\nu_{as}(CS)$	20, 23, 26
			327m	$\rho(CF_3)$ (cisoid)	20, 26
350s	$\rho(SO_3)$	27	341m	$\tau(SO_2)$ (transoid)	23
			402m	$\omega(SO_2)$	23
519w	$\delta_s(CF_3)$	27	552w	$\delta_s(SO_2)$	23
575m	$\delta_s(SO_3)$	27	573w	$\delta_{as}(CF_3)$, $\delta^{ip}{}_s(R)$	23
			589vw	$\delta_{as}(CF_3)$, $\delta^{ip}{}_{as}(SO_2)$, $\delta_s(NSO_2)$	
			627w	γ(R), δ(SNS)	23
760s	$\delta_s(CF_3)$	24, 28	660w	δ(SNS), ν(N−CH3)	23
			743vs	$\delta_s(CF_3)$	23
			917w	γ(CH)	23
1034s	$\nu_s(SO_3)$	24, 25, 27			
1173vw	$\nu_{as}(CF_3)$	14, 24	1136m	$\nu_s(SO_2)$	23
1228m	$\nu_s(CF_3)$	24	1244m	$\nu_s(CF_3)$	23
1298m	$\nu_{as}(SO_3)$	24			

[a]The given assignment is according to reports available in the literature. Relative Raman intensities of observed vibrational modes are indicated as vw, very weak; w, weak; m, medium; s, strong. Abbreviations: ν, stretching; δ, in plane bending; τ, twisting; ρ, rocking; γ, out of plane bending; ω, wagging; ip, in phase; op, out of phase; s, symmetric; as, asymmetric.

The TfO anion shows very strong Raman signatures at 315, 350, 760, and 1034 cm^{-1} (Figure 3 and Table 2), which are assigned to the stretching mode of C−S, the rocking mode of SO_3, the bending mode of CF_3, and the stretching mode of SO_3, respectively.[24,25,27] That these modes truly arise from the TfO anion is further confirmed by the Raman spectrum recorded for $NaCF_3SO_3$ dissolved in water, which due to the monatomic character of Na^+ only displays the vibrations associated with $SO_3CF_3^-$ (see Supporting Information Figure SI-1). The vibrational modes at 760 and 1034 cm^{-1} are sensitive to intermolecular interactions[28] and, along with the vibration of TFSI at 743 cm^{-1}, have been further analyzed upon addition of water.

In Figure 4A the Raman spectrum of pure C_2HImTFSI is compared with the Raman spectra recorded upon addition of water. This figure reveals that the mode at 743 cm^{-1} shows almost no change in position when the water concentration is increased. In addition, the low frequency region 240−430 cm^{-1} does not show significant changes in relative intensity, indicating also that the conformational equilibrium between the *cis* and the *trans* forms remains unaffected upon addition of water (see Supporting Information Figure SI-2). Thus, we can conclude that the TFSI anion is not influenced by water in the whole concentration range investigated here. This may seem inconsistent with previous studies that propose a specific H_2O−anion interaction.[18,29−33] However, we must emphasize that this interaction scheme has been proposed for aprotic ionic liquids of hydrophilic anions, and may not necessarily hold for a protic cation associated with an hydrophobic anion.

By contrast, the Raman spectra recorded upon addition of water to the PIL C_2HImTfO reveal a systematic shift for the CF_3 bending mode at ~760 cm^{-1} (Figure 4B) and the SO_3 stretching mode at ~1035 cm^{-1} (Figure 4C). These spectral regions have been further analyzed by a peak-fit procedure using one Voigt profile to model the CF_3 bending mode, and two Voigt functions in the region of the SO_3 stretching to account for the contribution of the cation at ~1029 cm^{-1}; see Figure 5. This assignment is supported by our Raman spectrum recorded for the $NaCF_3SO_3$ salt dissolved in water, for which the 1035 cm^{-1} feature could very well be fitted by one single Voigt component. Our analysis shows that the positions of both the CF_3 bending and SO_3 stretching modes shift to higher frequencies when water is added. (Note: The Raman spectral region 500−1000 cm^{-1} was also analyzed in detail; however, in this region the frequency shifts were either negligibly small (500−700 cm^{-1}) or the vibrational modes too weak to be accurately modeled (800−1000 cm^{-1}). This increase is about 1 cm^{-1} within the concentration range investigated and, although apparently small, is quantitatively in agreement with the results presented by Bodo et al., who also show a blue-shift for the Raman stretching frequency of the nitrate anion (NO_3^-) in the ionic liquid 1-butyl-ammonium nitrate (BAN) upon addition of water.[32] By covering a more extended water concentration range, these authors also show that this blue-shift is initially stronger but then attenuates in solutions with approximately five water molecules per ion pair. Accordingly, Bodo et al. show that by adding 25 water molecules per $[BA]^+[N]^-$ ion pair the frequency shift for the N−O_3 stretching is limited to ~4 cm^{-1}. The shift to higher frequencies that we observe upon addition

DOI: 10.1021/jp510691e
J. Phys. Chem. B 2015, 119, 1611−1622

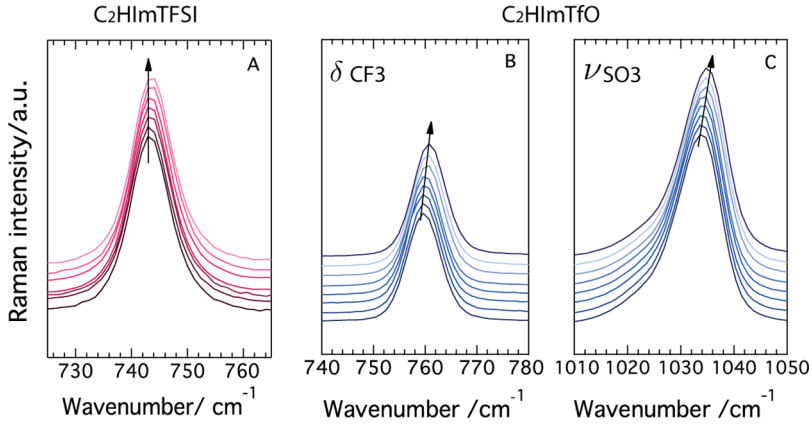

Figure 4. Raman spectra of C_2HImTFSI and C_2HImTfO. (A) Expansion−contraction mode of the TFSI anion in C_2HImTFSI. (B) Bending mode (δ) of CF_3. (C) stretching mode (υ_s) of SO_3 in C_2HImTfO as a function of water concentration. The black arrows indicate the increase of water concentration, from $x = 0$ to $x = 1$.

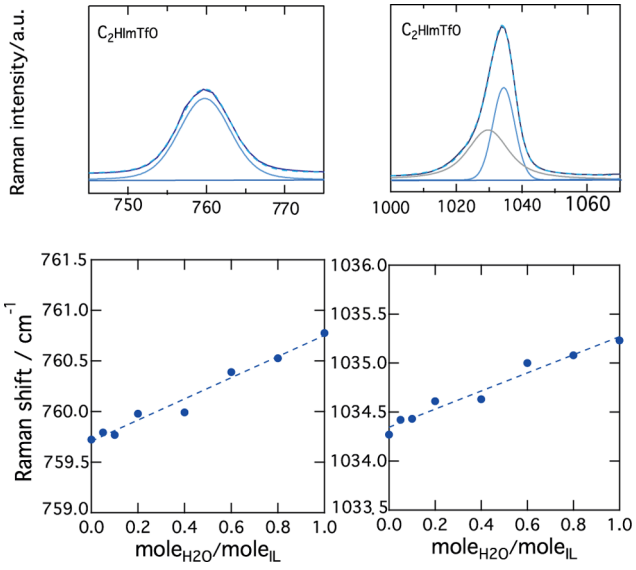

Figure 5. Top panel: peak fitting model for the CF_3 bending, and SO_3 stretching mode in C_2HImTfO. Bottom panel: Change in frequency for bending and stretching modes in C_2HImTfO as a function of water.

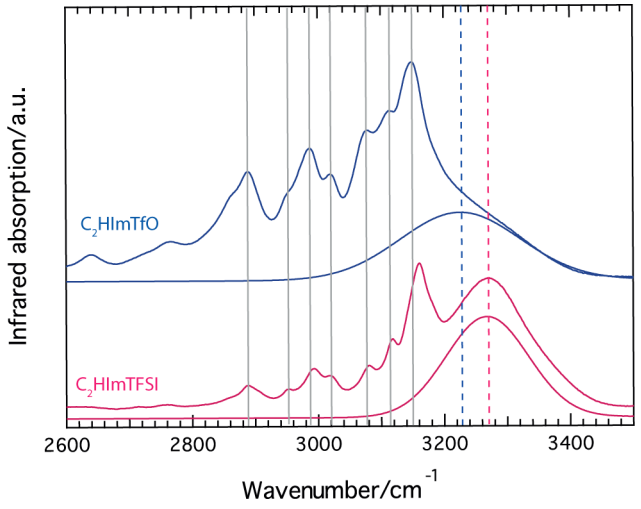

Figure 6. Infrared spectra of pure C_2HImTFSI (pink) and C_2HImTfO (blue) along with (N−H) stretching contribution to the spectra.The position of the N−H group is indicated by pink and blue dashed lines in two ionic liquids.

of water can be interpreted as the substitution of weak anion−cation interactions by slightly stronger anion−water interactions. Most likely these interactions are established through hydrogen bonding that, in the binary system H_2O/C_2HImTfO, may also involve the protic cation (vide infra). By contrast, the weaker propensity of the TFSI anion to interact with water (as deduced from the negligible changes in the whole Raman spectrum) can be rationalized by its basicity[34] and effective charge delocalization.

Vibrational Modes of the C_2HIm Cation. The IR spectra of C_2HImTFSI and C_2HImTfO are shown in Figure 6. The observed IR active vibrations are also summarized in Table 3 along with their assignments. It is interesting that most stretching modes of the −CH groups in the alkyl chain at frequencies between 2600 and 3000 cm^{-1} and in the imidazolium ring at frequencies between 3000 and 3150 cm^{-1} are found at the same position for the two PILs and at very similar positions to their aprotic counterparts (see Discussion in the preamble section). Nevertheless, while the N−H stretching mode in C_2HImTFSI is found at ∼3270 cm^{-1}, well separated from the C−H stretching modes, in C_2HImTfO this mode is observed at a lower frequency and appears as a broader feature underlying the C−H stretching envelope. A detailed peak-fit analysis in the wide frequency range 2500−4000 cm^{-1} shows that the N−H stretching is found at 3268 cm^{-1} for pure C_2HImTFSI and at 3231 cm^{-1} for pure C_2HImTfO (for more details on this fit procedure see Supporting Information Figure SI-3, Table SI-1, and Table SI-2). The frequency observed for the latter indicates a weak C_2HIm^+−TfO^- interaction, yet slightly stronger than the interaction between C_2HIm^+ and $TFSI^-$, in agreement with the results discussed above for the symmetric $C^{2,4,5}$−H stretching modes. This is also consistent with our previous NMR study that showed a chemical shift for the NH proton more downfield in C_2HImTfO than in C_2HImTFSI,[5] indicative of a stronger hydrogen bonding between the C_2HIm cation and the TfO anion. This is also in agreement with recent studies showing that although TFSI and TfO are both weak hydrogen-bond acceptors, TFSI is relatively weaker than TfO.[35]

Recently Cha et al. reported on the combined use of IR and ^{1}H NMR spectroscopy to investigate the nature of hydrogen bonding in aprotic imidazolium ionic liquids of the Cl^-, Br^-, I^-,

DOI: 10.1021/jp510691e
J. Phys. Chem. B 2015, 119, 1611−1622

Table 3. Observed Infrared Modes of C_2HImTfO and C_2HImTFSI at Room Temperature and Their Assignments According to the Literature[a]

C_2HImTfO			C_2HImTFSI		
ω (cm^{-1})	assignment	ref	ω (cm^{-1})	assignment	ref
757s	$\delta_s(CF_3)$	28	741	$\delta_s(CF_3)$, δ(R)	23
			764	ν_s(SNS), δ_{as}(HCCH)	23
911w	$\nu_{as}(CF_3)$	36	790	ν_s(CS), δ_{as}(HCCH)	23
			857	ν_{as}(SNS)	23
1026s	$\nu(SO_3)$	28	916	ν(R)	23
			1053	ν_s(R), ν_{as}(SNS)	23
1154vs	$\nu_s(CF_3)$	37	1085s	ν_s(CC), ν(R), δ(CH)	23
1223vs	$\nu_{as}(CF_3)$	37	1129vs	$\delta_s^{ip}(SO_2)$, $\nu_s(SO_2)$	23
			1178	ν_s(R), ν(N−CH_3), $\nu_{as}(CF_3)$	23
1277vs	$\nu_{as}(CF_3)$	27	1329	$\nu_{as}^{op}(SO_2)$, ν_s(R), ν(CC)	23
			1346vs	$\nu_{as}^{ip}(SO_2)$	23
1410w	$\nu_{as}(SO_2)$	36	1452m	$\delta_{as}(CH_3)$	23
1452m	$\delta_{as}(CH_3)$	23	1472m	$\delta_{as}(CH_3)$	23
1470m	$\delta_{as}(CH_3)$	23	1550m	ν(R)	23
1550s	ν(R)	23	1582m	$\nu_{s/as}^{ip}$(R), $\nu(CH_3)$, ν_s^{ip}(R)	23
1582s	$\nu_{s/as}^{ip}$(R), $\nu(CH_3)$, ν_s^{ip}(R)				
2889	$\nu_s(CH_3)$	19	2888	$\nu_s(CH_3)$	19
2989	$\nu_{as}(CH_3)$	19	2993	$\nu_{as}(CH_3)$	19
3022	$\nu_s(NCH_3)$	19	3016	$\nu_s(NCH_3)$	19
3070	$\nu(C^2H)$	19	3082	$\nu(C^2H)$	19
3109	$\nu_{as}(C^4HC^5H)$	19	3116	$\nu_{as}(C^4HC^5H)$	19
3149	$\nu_s(C^4HC^5H)$	19	3159	$\nu_s(C^4HC^5H)$	19

[a]Relative Raman intensity of observed vibrational modes are indicated as vw, very weak; w, weak; m, medium; s, strong. Abbreviations: ν, stretching; δ, in plane bending; τ, twisting; ρ, rocking; γ, out of plane bending; ω, wagging; ip, in phase; op, out of phase; s, symmetric; as, asymmetric.

and BF_4^- anion.[19] They have shown that stronger hydrogen bonding between the cation and the anion results in a more pronounced red-shift of the C−H stretching mode while the chemical shift of the corresponding CH proton appears more downfield. In their series, the strongest cation−anion interaction was observed in C_4C_1ImCl, and the weakest in $C_4C_1ImBF_4$. Their study also revealed that vibrational frequency changes of about 30−40 cm^{-1} reflect in relative chemical shifts of ∼1 ppm in the ^{1}H NMR spectrum. As Table 1 summarizes, the $C^{2,4,5}$−H stretching modes are found at systematically lower frequencies for the C_2HImTfO ionic liquid than for the C_2HImTFSI, and further indicate that the C_2HIm^+−TfO^- pair is in closer proximity than the C_2HIm^+−$TFSI^-$ counterpart. This is also supported by the calculated molar volumes of C_2HImTFSI and C_2HImTfO which are 240.3 and 173.4 cm^3/mol, respectively (Note: the molar volume (V_m) can be calculated using molar mass (M_w) and density (ρ) as follows: for C_2HImTFSI, $V_m = (M/\rho) = 377.28/1.57 = 240.28$ cm^3/mol, and for C_2HImTfO, $V_m = (M/\rho) = 246.21/1.42 = 173.38$ cm^3/mol). To summarize, among the ionic liquids reported in Table 1 the strength of cation−anion interaction increases in the order $C_4C_1ImBF_4 \approx C_2C_1$ImTFSI < C_2C_1ImTfO ≈ C_2HImTFSI < C_2HImTfO.

The effect of mixing PILs with water on the infrared spectra is illustrated in Figure 7, which shows the spectrum of

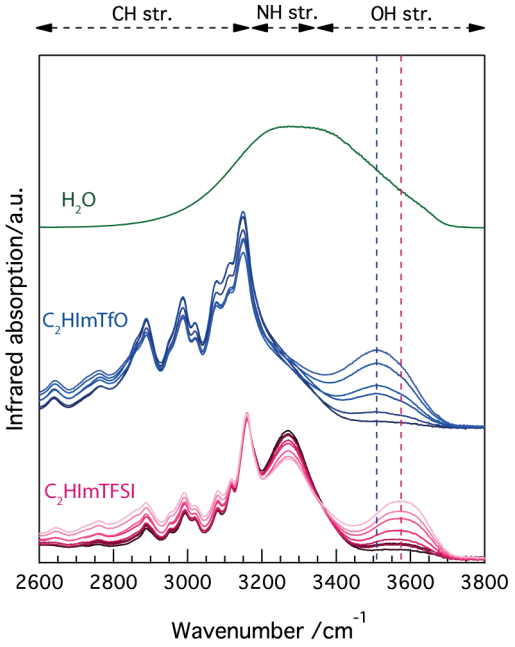

Figure 7. Effect of increasing water concentration observed by infrared spectra of the mixture of C_2HImTFSI (pink) and C_2HImTfO (blue) with water. The spectrum of pure water (green) is appended for comparison purpose.

molecular water (topmost trace) and of the H_2O/PILs binary systems for relative water contents ranging from $x = 0$ to $x = 1$. In this figure the regions typical of C−H stretching (2600−3150 cm^{-1}), N−H stretching (3150−3350 cm^{-1}), and O−H stretching (3400−3800 cm^{-1}) are indicated. In each spectral series, water content increases from bottom to top. While the signature assigned to O−H stretching (discussed further in the next section) increases with x, as expected, the signature at 3268 cm^{-1} attributed to the N−H stretching in C_2HImTFSI seems to decrease. This was also confirmed by the peak-fit analysis that revealed an intensity loss of about 20% for this mode when normalized to any of the ring or alkyl C−H stretching modes (Figure 8A). This effect is intriguing and deserves particular attention, since it involves the protic −NH group that has an important functionality in, for instance, fuel cell applications.

We know from our previous ^{1}H NMR study[5] that the proton on the −NH group exchanges with the protons of water, and we have also observed that the chemical shift of the NH proton, δ_{NH}, shifts downfield upon addition of water (see Figure 6 in ref 5). These findings indicate a molecular vicinity of water to the imidazolium cation as well as an NH−H_2O interaction, the nature of which has not been deciphered yet. If this interaction was a directional H-bonding between the NH proton and the oxygen of water, an elongation of the N−H bond would occur with a consequent shift to lower frequencies of the ν_{NH} mode, and possible broadening. Our analysis, however, shows very constant frequency values for this mode through the entire water concentration investigated (Figure 8B). Hence, the reduced integrated area of the ν_{NH} peak could in principle be explained by a dissociation of the protic imidazolium. Such a dissociation would reduce the number of −NH groups in solution and thus be consistent with the proportionality of the

DOI: 10.1021/jp510691e
J. Phys. Chem. B 2015, 119, 1611−1622

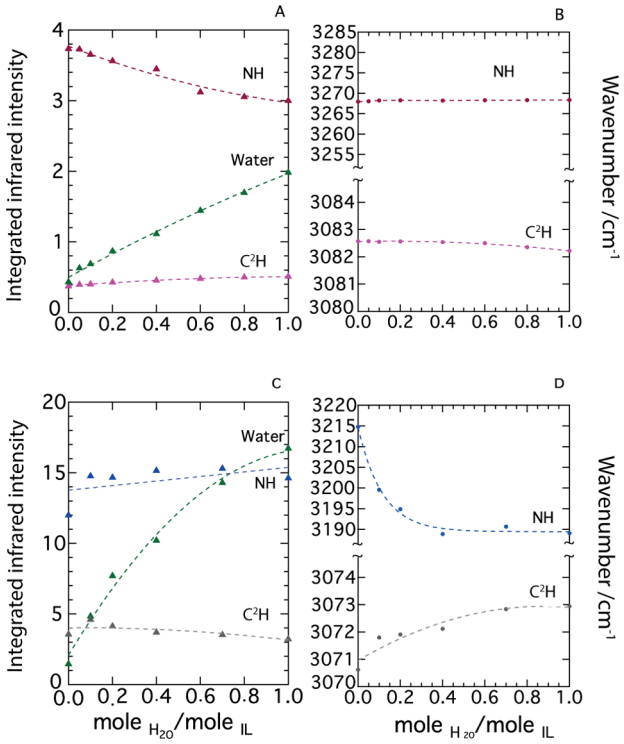

Figure 8. Integrated infrared intensities (A) and infrared frequencies (B) of the N−H, C^2−H, and O−H stretching modes for C_2HImTFSI as a function of water concentration. Intensities are normalized to the intensity of the C^7−H_3 stretching mode at 2889 cm^{-1}, which is thus used as an internal reference. Integrated infrared intensities (C) and frequencies (D) of the N−H, C^2−H, and O−H stretching modes for C_2HImTfO as a function of water concentration. Intensities are normalized to the intensity of the C^4HC^5H stretching mode at 3159 cm^{-1}.

IR intensity, I_{IR}, to the concentration of the vibrating species (recall that $I_{IR} \propto$ conc. × $\Delta\mu$, where $\Delta\mu$ is the change in the dipole moment associated with the vibration). However, we have some concerns in considering this alternative due to the following arguments. First of all, a full dissociation of some of the −NH groups would create free protons that should be found as either H_3O^+ or higher water complexes, such as $H_5O_2^+$. These should be observed at around 1710−1715 cm^{-1} and 1730−1750 cm^{-1}, respectively, in the infrared spectrum, but we could not detect any significant feature in this spectral range (see Supporting Information Figure SI-4). A free proton in the ionic liquid solution could also be found as a solvated species by $TFSI^-$, as recently observed by Yu et al. in mixtures of HTFSI and C_4C_1ImTFSI.[38] This solvated state would, however, strongly affect the shape and/or position of the TFSI characteristic mode at ∼743 cm^{-1}, which we do not observe (see Figure 4A). Additionally, the stability toward added water of the infrared absorptions at 1550 and 1580 cm^{-1} (assigned to the ring stretching modes R_1 and R_2 of the imidazolium)[39,40] in terms of intensity, shape, and position does not support proton dissociation either (see Supporting Information Figure SI-4). Finally, considerations about the pK_a of all species possibly providing proton donor−acceptor sites lead us to the conclusion that the C_2HIm cation is unlikely to liberate the proton from the −NH site (note: in this context we have used the following data reported by Angell et al.: pK_a [HIm^+] = 6.9, pK_a [H_3O^+] = 0, pK_a [HTFSI] ≃ −12.2[41]). Accordingly, the trends observed in the infrared spectrum as a function of added water must find another explanation.

Apart from the changes observed in the high-frequency range, that concern mainly absorption intensities, the only other effects on the infrared spectrum of C_2HImTFSI are detected in the frequency range 700−1000 cm^{-1}. According to the assignment scheme proposed by Grondin et al.[21,39] for diverse imidazolium ionic liquids, this region contains contribution from out-of-plane bending modes of the ring −CH groups, that is, the γ_{ip} $C^{4,5}H$ at ∼751 cm^{-1}, the γ C^2H at ∼820 cm^{-1}, and the γ_{op} $C^{4,5}H$ at ∼860 cm^{-1}. In the IR spectrum of C_2HImTFSI shown in Figure 9 the mode at ∼751

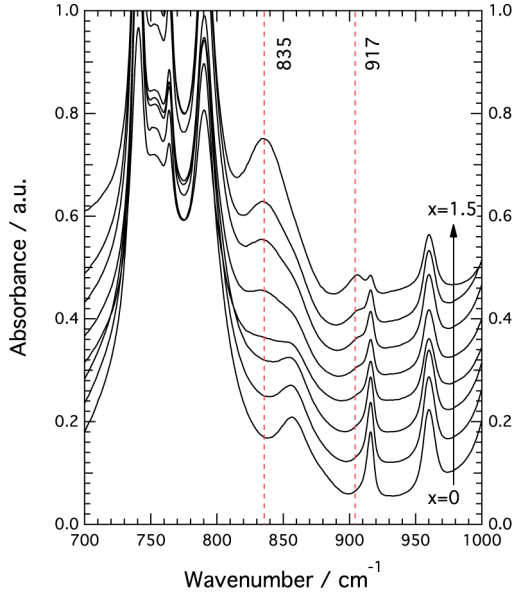

Figure 9. Infrared spectral region which contains the contribution of out-of-plane bending modes of the ring −CH groups.

cm^{-1} is submerged with the infrared signatures of the TFSI anion and the mode at ∼820 cm^{-1} appears very weak, while that at ∼860 cm^{-1} is well resolved. In addition, we observe a signature at 961 cm^{-1} assigned to C−C stretching in the alkyl group and characteristic of alkyl-imidazolium ionic liquids. Along with these features, we also detect an additional mode at ∼917 cm^{-1}, which is only present in the protic ionic liquids, i.e., in C_2HImTFSI and C_2HImTfO but not in C_2C_1ImTFSI and C_2C_1ImTfO, and vanishes in the deuterated form, i.e., in C_2DImTFSI (see Supporting Information Figure SI-5). To the best of our knowledge there are no reported assignment or published calculated vibrational spectra for PILs of the imidazolium cation; nevertheless, previous spectroscopic studies on imidazole and imidazolium at different complexation states[40,42] suggest that the feature at ∼917 cm^{-1} can tentatively be assigned to the out-of-plane bending mode of the −NH group, i.e., to γ NH. As a consequence, the appearance of a shoulder at ∼905 cm^{-1} and the concomitant enhancement of the ∼820 cm^{-1} mode with increasing water concentration (see Figure 9) may arise from a specific interaction of water with both the $-C^2H$ and the $-N^3H$ sites, with the water sharing its oxygen atom transversally to the C−H and N−H bond directions. This hypothetic coordination scheme is illustrated in Figure 10A.

The intensity increase of the signature at ∼820 cm^{-1} can be rationalized by the γ C^2H mode being activated by this new

DOI: 10.1021/jp510691e
J. Phys. Chem. B 2015, 119, 1611−1622

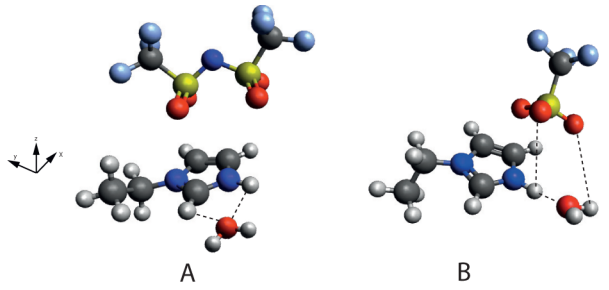

Figure 10. Hypothetic coordination scheme for water interacting with the cation in C_2HImTFSI (A) and with both cation and anion in C_2HImTfO (B).

interaction,[21] while its negligible intensity in the spectrum of the pure C_2HImTFSI would be a consequence of the weak and nonspecific C_2HIm^+−$TFSI^-$ interaction (note that one argument of Grondin et al.[21] for assigning the 820 cm^{-1} vibration to the γ C^2H mode was its disappearance upon dissolution of the ionic liquid C_2C_1ImBr in water, which reduces the specificity of the C^2H−Br interaction). In this interpretation, we assume that the interaction of water with the acidic protons of the ring affects the charge density around the C^2 and N^3 atoms in a way that the change in dipole moment during the N−H stretching decreases (compared to the case of no added water). This could explain the lower intensity of the mode at 3268 cm^{-1} despite the molecular integrity of the C_2HIm^+ cation. (Note: our detailed analysis of ^{1}H NMR data previously reported in ref 5 is strongly against the dissociation model and rather supports the integer C_2HIm^+ structure. In particular, the integrated NMR intensities associated with the cation and water in the H_2O/PIL binary system reveal that although proton exchange can occur the NH group does not lose its proton. This was also the conclusion drawn by comparing the self-diffusion values derived from the aromatic or aliphatic proton signals ($C^{2,4,5,6,7}$) with that obtained from the signal of the proton at the N^3H site.)

The spectroscopic signatures are slightly different for C_2HImTfO. First of all the peak-fit analysis reveals that the N−H stretching mode is found at a slightly lower frequency, i.e., at 3231 cm^{-1}, and has a broader character as compared to the case of TFSI. Upon addition of water, the N−H stretching mode maintains a constant intensity (when normalized to the intensity of the C^7−H_3 stretching mode at 2889 cm^{-1}, which is thus used as an internal standard) but shifts to lower frequencies; see Figure 8C and D. This indicates that the −NH group experiences classical hydrogen bonding that results in elongation of the N−H bond. By contrast, the C^2−H stretching modes slightly blue-shift with increased water concentration. Moreover, only minor changes are observed in the spectral range 700−1000 cm^{-1}, where the out-of-plane bending modes are observed; see Supporting Information Figure SI-5. The latter may indicate that in C_2HImTfO the C^2H site is not available for water interactions, probably because it already interacts with the TfO anion. This hypothesis may be supported by the observation that the ν C^2H mode is observed at 3070 cm^{-1} in C_2HImTfO and at 3082 cm^{-1} in C_2HImTFSI; see Table 1. The proposed coordination scheme between water and C_2HImTfO is shown in Figure 10B.

In summary, the vibrational signatures of both the cation and the anion are affected differently upon addition of water in the case of C_2HImTFSI and C_2HImTfO. Consequently, to better understand the complex nature of intermolecular interactions it becomes crucial to also investigate the state of water, which is appropriately done by inspection of the 3200−3800 cm^{-1} infrared spectral range where the O−H stretching modes are found. This will be the subject of the next section.

State of Water. In Figure 7 the O−H stretching modes assigned to water are clearly observed in the frequency range 3400−3800 cm^{-1}. Compared to molecular water, whose IR spectrum is shown in the same figure for comparison, these O−H stretching appear at higher frequencies and within a much narrower domain. This indicates that water molecules are separated from each other and exhibit a poorly extended H-bonding network. This is in agreement with some recently reported works on the state of water in alkyl-imidazolium ionic liquids,[43−45] which propose the existence of "free" water molecules. These studies, however, considered ionic liquids of

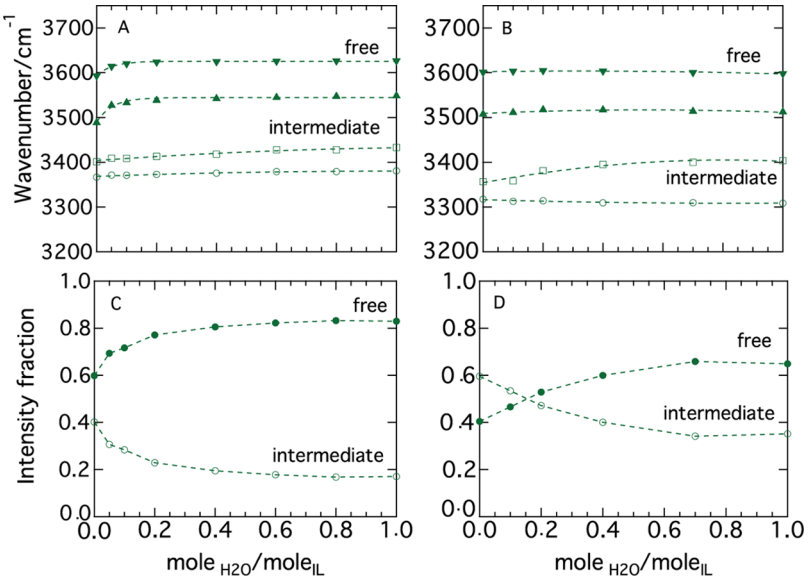

Figure 11. Frequency shift of "intermediate" and "free" water in C_2HImTFSI (A) and C_2HImTfO (B). Infrared intensity fraction of "free" and "intermediate" water in C_2HImTFSI (C) and C_2HImTfO (D).

DOI: 10.1021/jp510691e
J. Phys. Chem. B 2015, 119, 1611−1622

aprotic cations, while the state of water in protic imidazolium cations has to the best of our knowledge not been investigated before.

A closer inspection of Figure 7 also reveals that the vibrational modes assigned to water are found at relatively lower frequencies when added to C_2HImTfO than C_2HImTFSI; see vertical dotted lines. More specifically, the symmetric and asymmetric O−H stretching modes are found at 3515 and 3600 cm^{-1}, and at 3545 and 3625 cm^{-1}, respectively, in the 1/1 H_2O/PIL solutions; see Figure 11A and B. This difference along with the different band shape of the OH vibrations indicates that water is found in a slightly different configuration in C_2HImTfO compared to C_2HImTFSI. A similar conclusion was also drawn from the ^{1}H NMR chemical shift of the protons in H_2O when added to these PILs (see Supporting Information Figure SI-2 in ref 5).[5]

For TFSI we observed during the peak-fit procedure that to get a reasonable fit an additional feature had to be included to the left of the main envelope peaked at ∼3550 cm^{-1}, that is, at about 3380 cm^{-1}. In order to account for the symmetric (ν_s) and asymmetric (ν_{as}) stretching contributions of water, this feature has been modeled with two components, found at ∼3370 cm^{-1} and ∼3400 cm^{-1}, respectively (see also Supporting Information Figure SI-3). Modeling the infrared spectrum of water molecules added to an ionic liquid by two high-frequency components and one additional feature at ∼3400 cm^{-1} is in agreement with the works of Cammarata et al.,[43] Takamuku et al.,[18] and Fazio et al.[17] This low-frequency feature is thus assigned to more strongly bound water molecules (to either the anion or the cation, or both, depending on the molecular structure of the ionic liquid's ion pair). Since this frequency of vibration is lower than for "isolated" or "free" water molecules but still higher than for molecular water, which is characterized by an extended hydrogen-bonded network, these water molecules can appropriately be referred to as "intermediate".[17] Upon increasing water content, the relative contribution of intermediate water decreases, whereas that of isolated water dominates; see Figure 11C. This, along with the small but systematic blue-shift of all O−H stretching modes assigned to water suggests that in C_2HImTFSI added water tends to form separated nanodomains rather than to homogeneously dissolve within the ionic liquid network. As we will discuss in the next section, this is consistent not only with the phase behavior revealed by calorimetric measurements, but also with the observation that the mixture xH_2O/C_2HImTFSI with x = 2 displays phase separation. By contrast the xH_2O/C_2HImTfO system is homogeneously mixed up to at least x = 5.

For TfO, the wide spectral range 2500−3800 cm^{-1} has been peak-fitted with the same number of components as for C_2HImTFSI, including the two features assigned to "free" and "intermediate" water. The intermediate signatures are found at 3310 and 3400 cm^{-1} in the solution with one water molecule per ion pair (Figure 11B). In C_2HImTfO we observe that intermediate water initially contributes the most to the water signal, while for higher water concentrations the relative population of isolated molecules dominates (Figure 11D). Nevertheless, compared to the case of C_2HImTFSI, the contribution of intermediate water is greater.

To summarize, H_2O water is found in a state quite different from molecular water in both PILs investigated here, but in a slightly more hydrogen bonded network in C_2HImTfO. Judging from the analysis of concentration-dependent Raman spectra, this is due to the multiple and complex cation−water−anion interactions (see Figure 10B), whereas in C_2HImTFSI water interacts mainly with the cation, the anion being less affected. In other words, water seems to be more intimately mixed in C_2HImTfO, while it is more prone to phase separate in C_2HImTFSI.

Phase Behavior. Despite some recent works having addressed the effect of water on the chemico−physical properties of ionic liquids, such as density, viscosity, and heat of vaporization,[6−8] only one[46] has focused on how the phase behavior of protic ionic liquids changes as a function of added water. By performing calorimetric measurements we try here to relate the microscopic structure to the macroscopic properties, in particular, how these reflect in the glass transition and melting temperatures, T_g and T_m, respectively.

Figure 12 shows the DSC traces recorded upon heating for pure C_2HImTFSI and C_2HImTfO. The protic ionic liquid

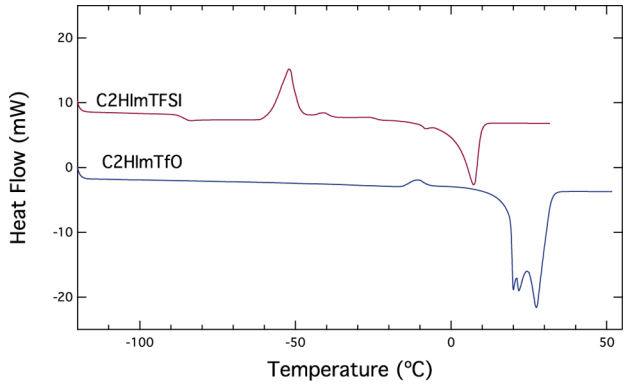

Figure 12. DSC traces of pure C_2HImTFSI and C_2HImTfO.

C_2HImTFSI displays a glass transition at −85.6 °C, followed by a cold crystallization process at −52 °C, and a relatively broad solid−liquid transition at ∼7 °C. Cold crystallization is typically observed in glass-forming liquids and polymers and, consistently with the detection of a T_g, indicates that the liquid does not crystallize upon cooling. This behavior has previously been observed in many other ionic liquids such as Pyr_{14}TFSI.[47−51] By contrast, C_2HImTfO easily crystallizes upon cooling (see Supporting Information Figure SI-6) and does not exhibit a glass transition or a cold crystallization on heating. Its melting is detected at ∼27 °C. These results suggest that the anion has a deep influence also on the phase behavior, and in particular that with TfO local ordering is promoted. In addition, the higher T_m value for C_2HImTfO reflects a stronger cation−anion interaction as compared to C_2HImTFSI, in full agreement with all spectroscopic results.

Upon addition of water the phase behavior of the two systems is affected in different ways; see Figure 13. For C_2HImTFSI, significant changes are observed already at very low water concentrations. For water contents $0.05 \leq x \leq 0.4$ major effects are observed in the melting, which displays several solid−solid transition peaks. These arise from the existence of several energetically close crystal phases. For water concentrations where $x \geq 0.5$, the melting appears as a single-peak again. To note, however, that the glass transition and the cold crystallization are observed for all water concentrations. Notably, for water contents $0.14 \leq x \leq 0.4$ a small crystallization peak is observed directly after T_g. The origin of this is not known, but could be related to some heterogeneities

DOI: 10.1021/jp510691e
J. Phys. Chem. B 2015, 119, 1611−1622

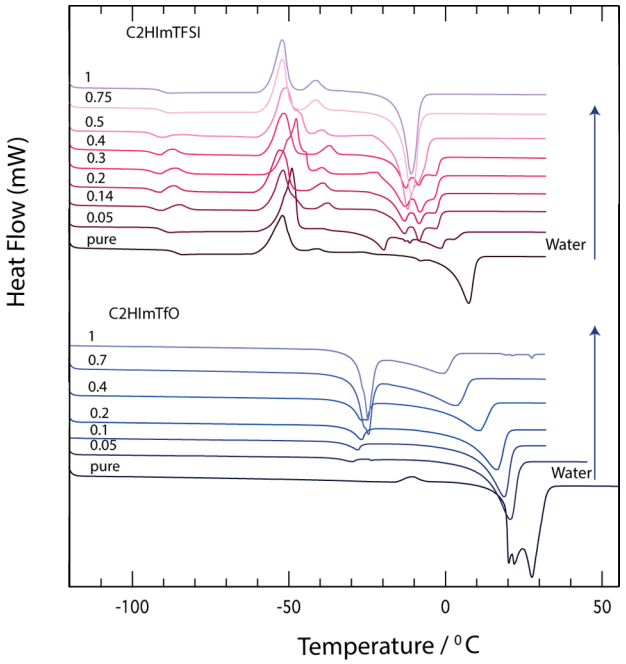

Figure 13. Phase behavior of $C_2HImTFSI$ and $C_2HImTfO$ binary system with water.

in the solution. For clarity, the changes in T_g and in T_m as a function of added water are summarized in Figure 14. The initial decrease of T_g can be attributed to a "plasticizing" effect of water, while the increase observed for $x \geq 0.3$ can be a consequence of a more extended hydrogen bonded network. A similar trend for T_g has recently reported by Elamin et al. for a xylitol–water binary system.[52]

For $C_2HImTfO$ the main changes upon addition of water consist of the appearance and increase of an additional phase transition peak at approximately −30 °C, and the shift to lower temperatures and decrease in enthalpy of fusion for the solid–liquid transition. This behavior can be attributed to a progressive decrease of the cation–anion cohesive forces and resembles that of eutectic mixtures (see also Supporting Information Figure SI-7, where an extended concentration range is included). This behavior is consistent with all other results discussed above and reflects the formation of an homogeneous solution where the water molecules and the C_2HIm^+ and TfO^- ions mutually interact. For more details on the phase behavior, see also Supporting Information Figure SI-8.

As summarized in Figure 14B, a common trend for $C_2HImTFSI$ and $C_2HImTfO$ is the overall decrease of the melting point (by ∼18 and 27 °C, respectively). (Note: the trend of the melting points for $C_2HImTFSI$ and $C_2HImTfO$ as a function of water are shown in more detail in Supporting Information Figure SI-8.) This implies a larger temperature window of the liquid state, which is beneficial for using PILs in fuel cells that operate at extreme conditions.

CONCLUSION

In this contribution we have investigated the effect of water on the local structure and phase behavior of the protic ionic liquids $C_2HImTfO$ and $C_2HImTFSI$, by employing vibrational spectroscopy (Raman and infrared) and differential scanning calorimetry (DSC).

We find that water coordinates differently in the two ionic liquids, interacting primarily with the cation in $C_2HImTFSI$ and mutually with both the cation and the anion in $C_2HImTfO$. This results in more homogeneous $H_2O/C_2HImTfO$ solutions, whereas the $H_2O/C_2HImTFSI$ binary system tends to form separated nanodomains, as also indicated by DSC. In addition, this different coordination causes water to be slightly more strongly H-bonded when mixed with $C_2HImTfO$, as reflected by the lower frequencies of the O–H stretching vibrations.

The greater ability of TfO to form hydrogen bonds (with both water and the cation) cannot be explained by acidity considerations only, since the pK_a of TfO has been reported to be lower than that of TFSI (pK_a TfO = −14, pK_a TFSI = −12.2).[41] This suggests that the ionic liquid polarity may be a more relevant parameter in predicting the degree of water association and thus the nature of H-bonding. According to the work of Rani et al.[53] the anion has the major impact on polarity that, for a given cation, is higher for TfO^- than for $TFSI^-$. That ionic liquids of the TfO anion are more polar than those of the TFSI anion is also concluded in the work of Köddermann et al.,[54] who demonstrate a linear correlation between the O–H stretching frequency of water (the solute) and the dielectric constant of the solvent (e.g., an ionic liquid). Plugging our O–H frequency values into their plot, we find that $C_2HImTfO$ exhibit a higher polarity than $C_2HImTFSI$ in agreement with

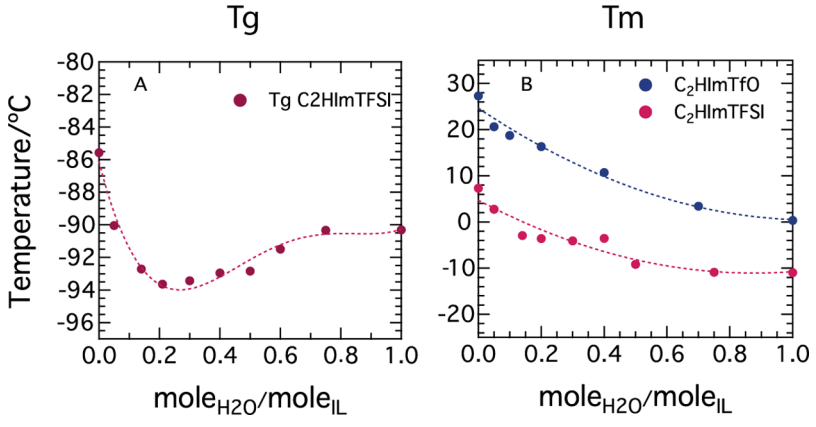

Figure 14. (A) Glass transition temperature of $C_2HImTFSI$ as a function of water. (B) Melting temperature of $C_2HImTFSI$ and $C_2HImTfO$ as a function of water.

DOI: 10.1021/jp510691e
J. Phys. Chem. B 2015, 119, 1611–1622

the discussion above and that, as expected, C_2HImTFSI is more polar than its aprotic counterpart C_2C_1ImTFSI.

These results provide new insights on the structural parameters that play a role in determining the nature of H-bonding in H_2O/PIL binary systems. These insights are of particular importance for the design of next-generation fuel cell electrolytes, whose performance depends on the mechanism of proton (H^+) transport.

■ ASSOCIATED CONTENT

Supporting Information

Additional Raman and Infrared spectra in complementary frequency ranges that support our results and discussion. Supplementary tables showing the results of the peak fitting procedure applied to the high frequency range of infrared spectra. Additional DSC traces and full phase diagram plots. This material is available free of charge via the Internet at http://pubs.acs.org.

■ AUTHOR INFORMATION

Corresponding Author

*E-mail: anna.martinelli@chalmers.se.

Notes

The authors declare no competing financial interest.

■ ACKNOWLEDGMENTS

Financial support from the Swedish Research Council, the Swedish Energy Agency, and the Chalmers' *Energy* and *Materials Science* Areas of Advance is kindly acknowledged. We also thank Prof. Doseok Kim for sharing the Infrared data of [C_4C_1ImBF$_4$] and [C_4C_1ImCl] ionic liquids.

■ REFERENCES

(1) Greaves, T. L.; Drummond, C. J. Protic Ionic Liquids: Properties and Applications. *Chem. Rev.* **2008**, *108*, 206−237.

(2) Earle, M. J.; Esperança, J. M. S. S.; Gilea, M. A.; Lopes, J. N. C.; Rebelo, L. P. N.; Magee, J. W.; Seddon, K. R.; Widegren, J. A. The Distillation and Volatility of Ionic Liquids. *Nature* **2006**, *439*, 831−834.

(3) O'Dea, J. R.; Economou, N. J.; Buratto, S. K. Surface Morphology of Nafion at Hydrated and Dehydrated Conditions. *Macromolecules* **2013**, *46*, 2267−2274.

(4) Kohno, Y.; Ohno, H. Ionic Liquid/Water Mixtures: From Hostility to Conciliation. *Chem. Commun.* **2012**, *48*, 7119−30.

(5) Yaghini, N.; Nordstierna, L.; Martinelli, A. Effect of Water on the Transport Properties of Protic and Aprotic Imidazolium Ionic Liquids - An Analysis of Self-Diffusivity, Conductivity, and Proton Exchange Mechanism. *Phys. Chem. Chem. Phys.* **2014**, *16*, 9266−9275.

(6) Seddon, K. R.; Stark, A.; Torres, M. Influence of Chloride, Water, and Organic Solvents on the Physical Properties of Ionic Liquids. *Pure Appl. Chem.* **2000**, *72*, 2275−2287.

(7) Domanska, U.; Rekawek, A.; Marciniak, A. Solubility of 1-Alkyl-3-Ethylimidazolium-Based Ionic Liquids in Water and 1-Octanol. *J. Chem. Eng. Data* **2008**, *53*, 1126−1132.

(8) Rodríguez, H.; Brennecke, J. F. Temperature and Composition Dependence of the Density and Viscosity of Binary Mixtures of Water + Ionic Liquid. *J. Chem. Eng. Data* **2006**, *51*, 2145−2155.

(9) Shao, Y.; Yin, G.; Wang, Z.; Gao, Y. Proton Exchange Membrane Fuel Cell from Low Temperature to High Temperature: Material Challenges. *J. Power Sources* **2007**, *167*, 235−242.

(10) Zhang, L.; Zhang, J.; Wilkinson, D. P.; Wang, H. Progress in Preparation of Non-Noble Electrocatalysts for PEM Fuel Cell Reactions. *J. Power Sources* **2006**, *156*, 171−182.

(11) Wang, B. Recent Development of Non-Platinum Catalysts for Oxygen Reduction Reaction. *J. Power Sources* **2005**, *152*, 1−15.

(12) Martinelli, A.; Iojoiu, C.; Sergent, N. A H_2/O_2 Fuel Cell for In Situ μ-Raman Measurements. In-Depth Characterization of an Ionic Liquid Filled Nafion Membrane. *Fuel Cells* **2012**, *12*, 169−178.

(13) Mori, K.; Kobayashi, T.; Sakakibara, K.; Ueda, K. Experimental and Theoretical Investigation of Proton Exchange Reaction between Protic Ionic Liquid Diethylmethylammonium Trifluoromethanesulfonate and H_2O. *Chem. Phys. Lett.* **2012**, *552*, 58−63.

(14) Chang, T. M.; Dang, L. X.; Devanathan, R.; Dupuis, M. Structure and Dynamics of N, N-Diethyl-N-Methylammonium Triflate Ionic Liquid, Neat and with Water, from Molecular Dynamics Simulations. *J. Phys. Chem. A* **2010**, 12764−12774.

(15) Li, W.; Zhang, Z.; Han, B.; Hu, S. Effect of Water and Organic Solvents on the Ionic Dissociation of Ionic Liquids. *J. Phys. Chem. B* **2007**, *111*, 6452−6456.

(16) Aleksa, V.; Kausteklis, J.; Klimavicius, V.; Gdaniec, Z.; Balevicius, V. Raman and NMR Spectroscopy Study of Liquid Crystalline Ionogel Phase in Ionic Liquid/H_2O Mixtures: The States of Water. *J. Mol. Struct.* **2011**, *993*, 91−96.

(17) Fazio, B.; Triolo, A.; Marco, G. D. Local Organization of Water and Its Effect on the Structural Heterogeneities in Room-Temperature Ionic Liquid/H_2O Mixtures. *J. Raman Spectrosc.* **2008**, 233−237.

(18) Takamuku, T.; Kyoshoin, Y.; Shimomura, T.; Kittaka, S. Effect of Water on Structure of Hydrophilic Imidazolium-Based Ionic Liquid. *J. Phys. Chem. B* **2009**, *113*, 10817−10824.

(19) Cha, S.; Ao, M.; Sung, W.; Moon, B.; Ahlström, B.; Johansson, P.; Ouchi, Y.; Kim, D. Structures of Ionic Liquid-Water Mixtures Investigated by IR and NMR Spectroscopy. *Phys. Chem. Chem. Phys.* **2014**, *16*, 9591−9601.

(20) Herstedt, M.; Smirnov, M.; Johansson, P.; Chami, M.; Grondin, J.; Servant, L.; Lassègues, J. C. Spectroscopic Characterization of the Conformational States of the Bis(trifluoromethanesulfonyl)imide Anion (TFSI-). *J. Raman Spectrosc.* **2005**, *36*, 762−770.

(21) Grondin, J.; Lassègues, J.-C.; Cavagnat, D.; Buffeteau, T.; Johansson, P.; Holomb, R. Revisited Vibrational Assignments of Imidazolium-Based Ionic Liquids. *J. Raman Spectrosc.* **2011**, *42*, 733−743.

(22) Fumino, K.; Peppel, T.; Geppert-Rybczynska, M.; Zaitsau, D. H.; Lehmann, J. K.; Verevkin, S. P.; Köckerling, M.; Ludwig, R. The Influence of Hydrogen Bonding on the Physical Properties of Ionic Liquids. *Phys. Chem. Chem. Phys.* **2011**, *13*, 14064−14075.

(23) Moschovi, A. M.; Ntais, S.; Dracopoulos, V.; Nikolakis, V. Vibrational Spectroscopic Study of the Protic Ionic Liquid 1-H-3-Methylimidazolium Bis(trifluoromethanesulfonyl)imide. *Vib. Spectrosc.* **2012**, *63*, 350−359.

(24) Huang, W.; Frech, R.; Wheeler, R. A. Molecular Structures and Normal Vibrations of CF_3SO_3 and Its Lithium Ion Pairs and Aggregates. *J. Phys. Chem.* **1994**, 100−110.

(25) Schantz, S.; Sandahl, J.; Börjesson, L. B. I.; Torell, L. M.; Stevens, J. R. Ion Pairing in Polymer Electrolytes; A Comparative Raman Study of $NaCF_3SO_3$ Complexed in Poly (Propylene-Glycol) and Dissolved in Acetonitrile. *Solid State Ionics* **1988**, *30*, 1047−1053.

(26) Martinelli, A.; Matic, A.; Johansson, P.; Jacobsson, P.; Börjesson, L.; Fernicola, A.; Panero, S.; Scrosati, B.; Ohno, H. Conformational Evolution of $TFSI^-$ in Protic and Aprotic Ionic Liquids. *J. Raman Spectrosc.* **2011**, *42*, 522−528.

(27) Cooney, R. P. Raman and Infrared Spectra and Normal Coordinates of the Trifluoromethanesulfonate and Trichloromethanesulfonate Anions. *Spectrochem Acta* **1969**, *25A*, 1515−1526.

(28) Burba, C. M.; Rocher, N. M.; Frech, R. Hydrogen-Bonding and Ion-Ion Interactions in Solutions of Triflic Acid and 1-Ethyl-3-Methylimidazolium Triflate. *J. Phys. Chem. B* **2009**, *113*, 11453−11458.

(29) Menjoge, A.; Dixon, J.; Brennecke, J. F.; Maginn, E. J.; Vasenkov, S. Influence of Water on Diffusion in Imidazolium-Based Ionic Liquids: A Pulsed Field Gradient NMR Study. *J. Phys. Chem. B* **2009**, *113*, 6353−6359.

(30) Spohr, H. V.; Patey, G. N. The Influence of Water on the Structural and Transport Properties of Model Ionic Liquids. *J. Chem. Phys.* **2010**, *132*, 2345101−2345113.

DOI: 10.1021/jp510691e
J. Phys. Chem. B 2015, 119, 1611−1622

(31) Grishina, E.; Ramenskaya, L.; Gruzdev, M.; Kraeva, O. Water Effect on Physicochemical Properties of 1-Butyl-3-Methylimidazolium Based Ionic Liquids with Inorganic Anions. *J. Mol. Liq.* **2013**, *177*, 267−272.
(32) Bodo, E.; Mangialardo, S.; Capitani, F.; Gontrani, L.; Leonelli, F.; Postorino, P. Interaction of a Long Alkyl Chain Protic Ionic Liquid and Water. *J. Chem. Phys.* **2014**, *140*, 2045031−10.
(33) Singh, T.; Kumar, A. Cation-Anion-Water Interactions in Aqueous Mixtures of Imidazolium Based Ionic Liquids. *Vib. Spectrosc.* **2011**, *55*, 119−125.
(34) Bonhôte, P.; Dias, A. P.; Armand, M.; Papageorgiou, N.; Kalyanasundaram, K.; Grätzel, M. Hydrophobic, Highly Conductive Ambient-Temperature Molten Salts. *Inorg. Chem.* **1996**, *35*, 1168−1178.
(35) Cláudio, A. F. M.; Swift, L.; Hallett, J. P.; Welton, T.; Coutinho, J. A. P.; Freire, M. G. Extended Scale for the Hydrogen-Bond Basicity of Ionic Liquids. *Phys. Chem. Chem. Phys.* **2014**, *16*, 6593−6601.
(36) Edwards, H. G. M. The Vibrational Spectrum of Trifluoromethanesulphonic Acid, CF_3SO_3H, and the Determination of Its Degrees of Dissociation in Aqueous Solution by Raman Spectroscopy. *Spectrochim. Acta* **1989**, *45A*, 715−719.
(37) Varetti, E. L. The Infrared Spectra of Trifluoromethanesulphonic States of Aggregation. *Spectrochem. Acta.* **1988**, *44A*, 733−738.
(38) Yu, L.; Pizio, B. S.; Vaden, T. D. Conductivity and Spectroscopic Investigation of Bis(trifluoromethanesulfonyl)imide Solution in Ionic Liquid 1-Butyl-3-Methylimidazolium Bis(trifluoromethanesulfonyl)-imide. *J. Phys. Chem. B* **2012**, *116*, 6553−6560.
(39) Lasségues, J.-C.; Grondin, J.; Cavagnat, D.; Johansson, P. New Interpretation of the CH Stretching Vibrations in Imidazolium-Based Ionic Liquids. *J. Phys. Chem. A* **2009**, *113*, 6419−6421.
(40) Bellocq, A.-M.; Garrigou-Lagrange, C. Spectres de Vibration de Quelques Sels D'Imidazolium et D'Imidazolium (D2)1,3. *Spectrochim. Acta* **1971**, *27A*, 1091−1104.
(41) Angell, C. A.; Ansari, Y.; Zhao, Z. Ionic Liquids: Past, Present and Future. *Faraday Discuss.* **2012**, *154*, 9−27.
(42) Bonsor, D. H.; Borah, B.; Dean, R. L.; Wood, J. L. Complex Hydrogen Bonded Cations. The Imidazole/Imidazolium Complex Cation. *Can. J. Chem.* **1976**, *54*, 2458−2464.
(43) Cammarata, L.; Kazarian, S. G.; Salter, P. A.; Welton, T. Molecular States of Water in Room Temperature Ionic Liquids. *Phys. Chem. Chem. Phys.* **2001**, *3*, 5192−5200.
(44) Greaves, T. L.; Kennedy, D. F.; Weerawardena, A.; Tse, N. M. K.; Kirby, N.; Drummond, C. J. Nanostructured Protic Ionic Liquids Retain Nanoscale Features in Aqueous Solution While Precursor Brønsted Acids and Bases Exhibit Different Behavior. *J. Phys. Chem. B* **2011**, *115*, 2055−2066.
(45) Prouzet, E.; Brubach, J. B.; Roy, P. Differential Scanning Calorimetry Study of the Structure of Water Confined within AOT Lamellar Mesophases. *J. Phys. Chem. B* **2010**, *114*, 8081−8088.
(46) Chen, Z.; Greaves, T. L.; Fong, C.; Caruso, R. a.; Drummond, C. J. Lyotropic Liquid Crystalline Phase Behaviour in Amphiphile-Protic Ionic Liquid Systems. *Phys. Chem. Chem. Phys.* **2012**, *14*, 3825−3836.
(47) Martinelli, A.; Matic, A.; Jacobsson, P.; Börjesson, L.; Fernicola, A.; Scrosati, B. Phase Behavior and Ionic Conductivity in Lithium Bis(trifluoromethanesulfonyl)imide-Doped Ionic Liquids of the Pyrrolidinium Cation and Bis(trifluoromethanesulfonyl)imide Anion. *J. Phys. Chem. B* **2009**, *113*, 11247−11251.
(48) Henderson, W. A.; Passerini, S. Phase Behavior of Ionic Liquid-LiX Mixtures: Pyrrolidinium Cations and $TFSI^-$ Anions. *Chem. Mater.* **2004**, 2881−2885.
(49) Pitawala, J.; Scheers, J.; Jacobsson, P.; Matic, A. Physical Properties, Ion-Ion Interactions, and Conformational States of Ionic Liquids with Alkyl-Phosphonate Anions. *J. Phys. Chem. B* **2013**, *117*, 8172−8179.
(50) Gomez, E.; Calvar, N.; Dom, A.; Macedo, A. Thermal Analysis and Heat Capacities of 1-Alkyl-3-Methylimidazolium Ionic Liquids with NTf2, TfO, and DCA Anions. *Ind. Eng. Chem. Res.* **2013**, *52*, 2103−2110.
(51) Fredlake, C. P.; Crosthwaite, J. M.; Hert, D. G.; Aki, S. N. V. K.; Brennecke, J. F. Thermophysical Properties of Imidazolium-Based Ionic Liquids. *J. Chem. Eng. Data* **2004**, *49*, 954−964.
(52) Elamin, K.; Sjöström, J.; Jansson, H.; Swenson, J. Calorimetric and Relaxation Properties of Xylitol-Water Mixtures. *J. Chem. Phys.* **2012**, *136*, 1045081−1045088.
(53) Ab Rani, M. A.; Brant, A.; Crowhurst, L.; Dolan, A.; Lui, M.; Hassan, N. H.; Hallett, J. P.; Hunt, P. A.; Niedermeyer, H.; Perez-Arlandis, J. M.; et al. Understanding the Polarity of Ionic Liquids. *Phys. Chem. Chem. Phys.* **2011**, *13*, 16831−16840.
(54) Köddermann, T.; Wertz, C.; Heintz, A.; Ludwig, R. The Association of Water in Ionic Liquids: A Reliable Measure of Polarity. *Angew. Chem. Int. ed.* **2006**, *45*, 3697−3702.

DOI: 10.1021/jp510691e
J. Phys. Chem. B 2015, 119, 1611−1622